AppliedPhotophysics

# Determination of species-specific rate constants of the reaction between Ferrate(VI) and sulfonamide antibiotics


## Summary

For almost a century since penicillin's discovery in 1928 antibiotics have been used to treat infections in both humans and animals. Due to an ever increasing and aging population the use of antibiotics has increased. Large portions of antibiotics are unmetabolized and excreted as waste, entering the environment, and posing several risks to human and ecological health. Antibiotic-resistant bacteria and antibiotic-resistant genes, along with food and water contamination, are perhaps the biggest dangers faced if antibiotics continue to be overused. It is predicted that by 2050 over 10 million people will die of antibiotic resistant infections [1].


One group of antibiotics that have been widely used and may become a health hazard are the sulfonamides (SAs). SA antibiotics contain an aniline ring and a *N*-containing heterocyclic aromatic ring (R) joined by a sulfonamide linkage (**Figure 1**). These drugs have been extensively researched, with particular focus on ways to eliminate SAs in the water treatment industry. One method is to utilize the oxidation of SAs by ferrate(VI) ($Fe^{VI}O_4^{2-}$, $Fe^{VI}$) species. The results of a kinetic study of this pathway are discussed in this application note.

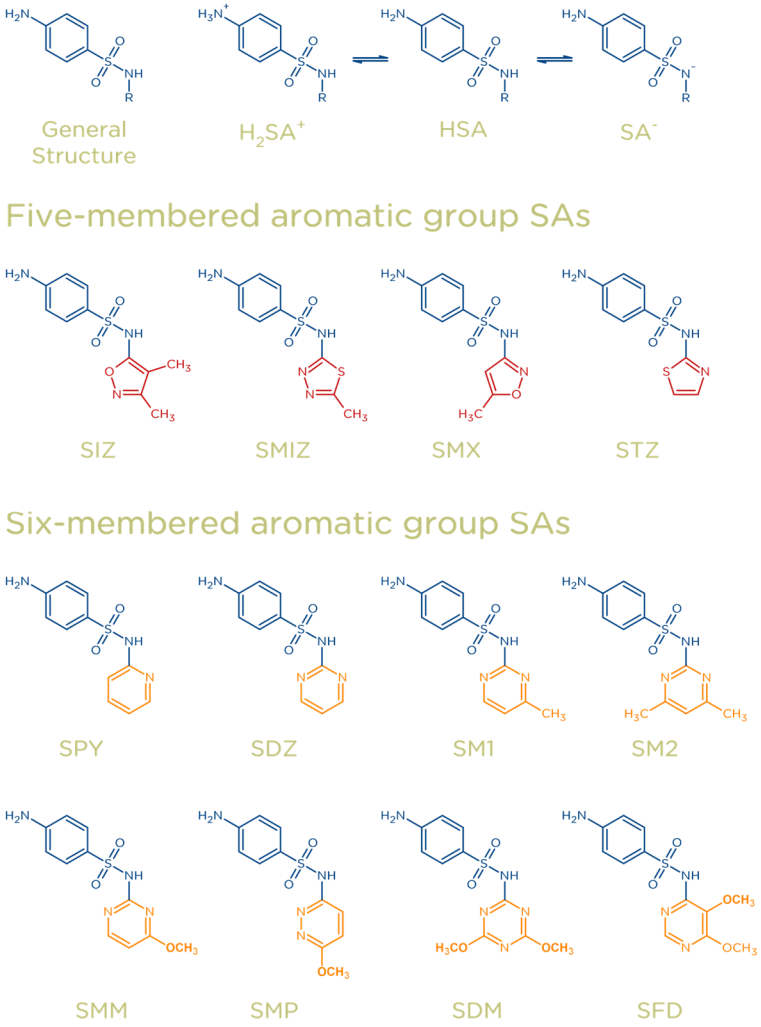


**Figure 1:** General structure of sulfonamide antibiotics (SAs) and structures of SAs with differing heterocyclic aromatic rings.

## Results & Discussion

**Figure 2** shows a plot of the resultant rate constants across the range of pH levels investigated in this study. The plot shows that as the pH of the reaction is increased from 6.5 – 10.0, the rate of reaction decreases, suggesting the sulfur dioxide extrusion in certain SAs is aided by protonation of the aniline species.

Within the acid-base equilibrium of the SAs and $Fe^{VI}$ at the pH range being tested only monoprotonated and unprotonated species of $Fe^{VI}$ and SAs were involved. It was observed that only two of the possible four reactions were needed to reasonably fit the experimental data, represented as equations 1 and 2 below:

$$HFeO_4^- + HX \xrightarrow{k_1} \text{Products} \quad (1)$$

$$FeO_4^{2-} + HX \xrightarrow{k_2} \text{Products} \quad (2)$$

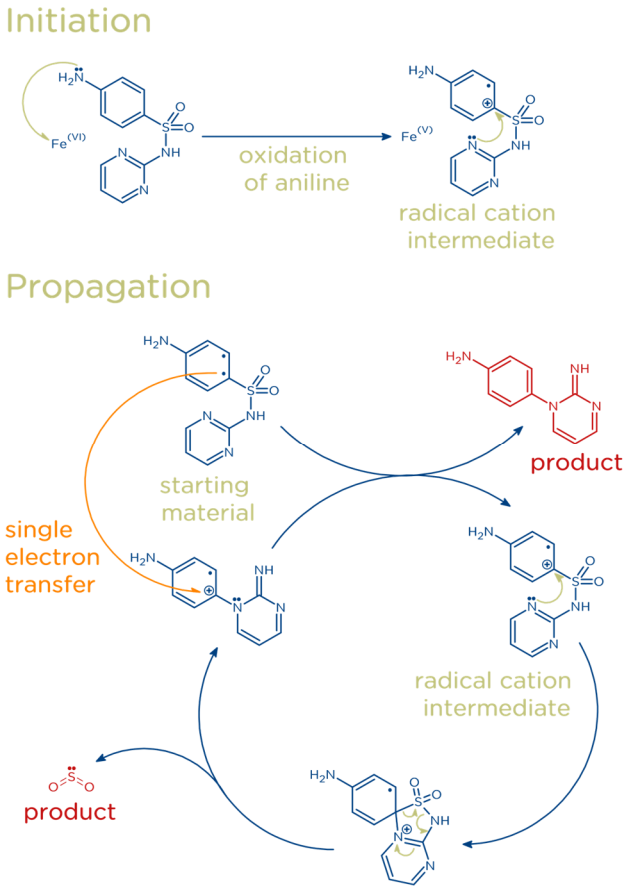


**Figure 3:** Mechanism for $Fe^{VI}$ catalysed extrusion of $SO_2$ from SDZ and other SAs.

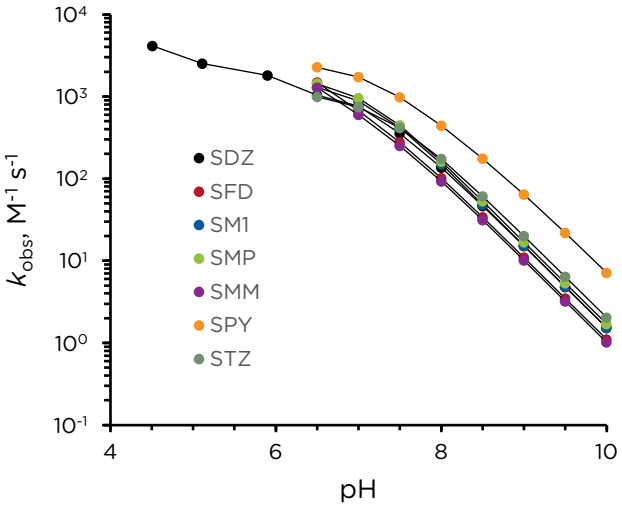


**Figure 2:** The observed second-order rate constants ($k_{obs}$, $M^{-1}s^{-1}$) is affected by pH for the oxidation of SAs by $Fe^{VI}$ at 25 °C. Recorded on a SX20 stopped-flow spectrometer.

It was deduced that the variation in $k_1$ is determined by the amount of influence the R moiety has on the aniline group, the site of $Fe^{VI}$ attack during SA oxidation.

Sulfadiazine (SDZ) was studied at an extended pH range down to 4.5, allowing the reaction between diprotonated $Fe^{VI}$ ($H_2FeO_4$) and protonated SDZ to be studied. Results show that the reaction of $Fe^{VI}$ and protonated SDZ species has the following order of reactivity:

All SA's tested in this study followed the same order,

$$H_2FeO_4 > HFeO_4^- > FeO_4^{2-}$$

showing that protonated $Fe^{VI}$ reacted faster than unprotonated $Fe^{VI}$ (i.e., $k_1 > k_2$). One explanation of this is that the partial radical character of $Fe^{VI}$ is stabilized by the presence of protons, meaning slower reaction rates in unprotonated species. In addition, the oxo-ligands in the protonated species of $Fe^{VI}$ have a larger spin density than the unprotonated species resulting to increased oxidative ability in the protonated $Fe^{VI}$.

As pH increases the ratio of protonated to unprotonated $Fe^{VI}$ decreases, resulting in the slower reaction rates which we see in **Figure 2**.

It was found that upon oxidation of the SAs containing a six-membered R group, sulfur dioxide was released as an oxidized product. However, no $SO_2$ extrusion was observed in SAs that contained a five-

 

membered ring. In the oxidation of SDZ, which has a six membered ring, two possible reaction pathways were proposed. One pathway suggested a single electron transfer to $Fe^{VI}$ from the aniline ring while the other, is an electron transfer from the R group (pyrimidine ring). Transition state calculations and analysis of the oxidation products *via* LC/MS techniques, support the former and suggest the R group is not involved in the initial SA oxidation by $Fe^{VI}$. The mechanism for this reaction pathway can be seen in **Figure 3**.

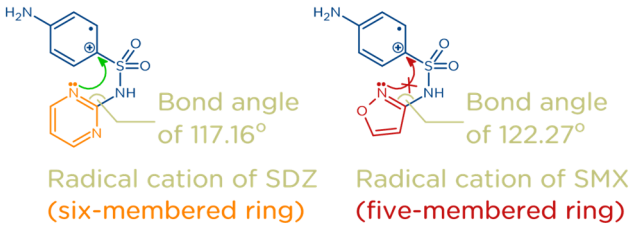


**Figure 4:** Difference in geometries between the five-membered ring in SMX and the six-membered ring in SDZ.

As previously stated, this mechanism is unique in SAs containing a six-membered ring, but this ring must also contain a nitrogen atom which is ortho to the amido nitrogen. The presence of this nitrogen in the ring allows for the formation of a five-membered ring intermediate, as shown in the **Figure 3**. The formation of this intermediate removes the aromaticity of the aniline ring, and the final step extruding SO2 restores this aromaticity.

Although this reaction is happening in the presence of $Fe^{VI}$, this is just initi ating the catalytic cycle. The extrusion of $SO_2$ also forms another radical cation intermediate which initiates the oxidation of another SA molecule, starting the propagation of further reaction.

A key question is why does this occur in six-membered rings but not in five-membered rings? Six-membered rings lead to the extrusion of $SO_2$ as the geometry allows the lone pair on one of the nitrogen atoms to be donated into the heterocyclic radical. In the case of a five membered ring the lone pair cannot be donated as due to the geometry the lone pair is too far away from the radical to be donated as can be seen in **Figure 4**. More electron donating R groups increase the nucleophilic activity of the aniline group which attacks the $Fe^{VI}$ species.

## Conclusion

Applied Photophysics SX20 stopped-flow spectrometer can be used to study the species-specific rate constants of the reactions between $Fe^{VI}$ and SAs. Values of *k* at pH 7.0 and 8.0 were used to learn the half-lives of the elimination of SAs by $Fe^{VI}$. For the practical application of this work, if $Fe^{VI}$ concentration is in excess at pH 8.0 and 25.0 °C then the removal of SAs would be short and in the range of 12.52 – 361.20 s depending on the SA species. Due to the dependence of this oxidation reaction on $Fe^{VI}$ concentration and pH, application conditions could be fine tuned to majorly reduce time spent in the removal of SAs.

## Methods

**Absorbance Stopped-Flow.** The oxidation of seven SAs (**Figure 1**) by $Fe^{VI}$ was studied at varying pH levels between 6.5 and 10.0. The rate constant $k_{obs}$ at these various pH levels was determined using a SX20 stopped-flow spectrometer, fitted with an absorbance photomultiplier tube detector. The light source was a xenon arc non-ozone producing lamp with absorbance recorded at 510 nm. Rate constants for oxidation of each SA were calculated using Applied Photophysics Pro-KIV software to analyse an average of six kinetic traces. Pseudo-first-order conditions were created by putting the SA concentration in a ten-fold excess.

In some cases, identification of oxidized products (OPs) was carried out via solid phase extraction liquid chromatography high resolution mass spectrometry (SPE-LC-HRMS). For more details refer to [2].

## References

1. https://www.economist.com/graphic-detail/2018/04/02/antibiotic-use-is-rapidly-increasing-in-developing-countries, accessed 07th October 2020
2. M. Feng, J. C. Baum, N. Nesnas, Y. Lee, C.-H. Huang, and V. K. Sharma, 2019, *Environ. Sci. Technol.*, 53, 2695–2704.

 